

THE OFFICIAL MAGAZINE OF THE OCEANOGRAPHY SOCIETY

Oceanography

CITATION

Embley, R.W., Y. Tamura, S.G. Merle, T. Sato, O. Ishizuka, W.W. Chadwick Jr., D.A. Wiens, P. Shore, and R.J. Stern. 2014. Eruption of South Sarigan Seamount, Northern Mariana Islands: Insights into hazards from submarine volcanic eruptions. *Oceanography* 27(2):24–31, <http://dx.doi.org/10.5670/oceanog.2014.37>.

DOI

<http://dx.doi.org/10.5670/oceanog.2014.37>

COPYRIGHT

This article has been published in *Oceanography*, Volume 27, Number 2, a quarterly journal of The Oceanography Society. Copyright 2014 by The Oceanography Society. All rights reserved.

USAGE

Permission is granted to copy this article for use in teaching and research. Republication, systematic reproduction, or collective redistribution of any portion of this article by photocopy machine, reposting, or other means is permitted only with the approval of The Oceanography Society. Send all correspondence to: info@tos.org or The Oceanography Society, PO Box 1931, Rockville, MD 20849-1931, USA.

Eruption of South Sarigan Seamount, Northern Mariana Islands

Insights into Hazards from Submarine Volcanic Eruptions

BY ROBERT W. EMBLEY, YOSHIHIKO TAMURA, SUSAN G. MERLE,
TOMOKI SATO, OSAMU ISHIZUKA, WILLIAM W. CHADWICK JR.,
DOUGLAS A. WIENS, PATRICK SHORE, AND ROBERT J. STERN

ABSTRACT. The eruption of South Sarigan Seamount in the southern Mariana arc in May 2010 is a reminder of how little we know about the hazards associated with submarine explosive eruptions or how to predict these types of eruptions. Monitored by local seismometers and distant hydrophones, the eruption from ~ 200 m water depth produced a gas and ash plume that breached the sea surface and rose ~ 12 km into the atmosphere. This is one of the first instances for which a wide range of pre- and post-eruption observations allow characterization of such an event on a shallow submarine volcanic arc volcano. Comparison of bathymetric surveys before and after the eruptions of the South Sarigan Seamount reveals the eruption produced a 350 m diameter crater, deeply breached on the west side, and a broad apron downslope with deposits > 50 m thick. The breached summit crater formed within a pre-eruption dome-shaped summit composed of andesite lavas. Dives with the Japan Agency for Marine-Earth Science and Technology *Hyper-Dolphin* remotely operated vehicle sampled the wall of the crater and the downslope deposits, which consist of andesite lava blocks lying on pumiceous gravel and sand. Chemical analyses show that the andesite pumice is probably juvenile material from the eruption. The unexpected eruption of this seamount, one of many poorly studied shallow seamounts of comparable size along the Mariana and other volcanic arcs, underscores our lack of understanding of submarine hazards associated with submarine volcanism.

AN UNUSUAL ERUPTION ON THE MARIANA ARC

An unexpected submarine volcanic eruption on the southern Mariana arc (Figure 1a,b) in 2010 provides insights into the volcanic processes of submarine eruptions and the hazards these hidden volcanoes pose. On May 28–29, 2010,

an underwater eruption occurred on South Sarigan Seamount, a poorly surveyed submarine volcano lying between Sarigan and Anatahan Islands in the Commonwealth of the Northern Mariana Islands (Figure 1a,b). The eruption was unusual because this seamount had no known historical

activity. Seismic body waves and T-phases (waterborne acoustic waves) produced by the eruptive events were recorded on seismometers on nearby islands (Searcy, 2013) and on submarine hydrophones and seismometers located 2,260 km to the east of South Sarigan Seamount. The mid-Pacific instruments near Wake Island are operated by the International Monitoring System (IMS) of the Comprehensive Nuclear Test Ban Treaty (CTBT) (Green et al., 2013). Precursory volcano-tectonic earthquakes began in early April 2010 and continued intermittently through April and early May, with a significant increase in size and number of swarms beginning on May 11 (Searcy, 2013). Hydroacoustic phases, interpreted as eruptive activity (Green et al., 2013; Searcy, 2013), began on May 27, reaching a peak during a three-hour period early on May 29 with near-continuous volcanic tremor. Also during this time span, patches of discolored water were observed on the ocean surface (McGimsey et al., 2010) and infrasound events (atmospheric acoustic signals) were recorded on a

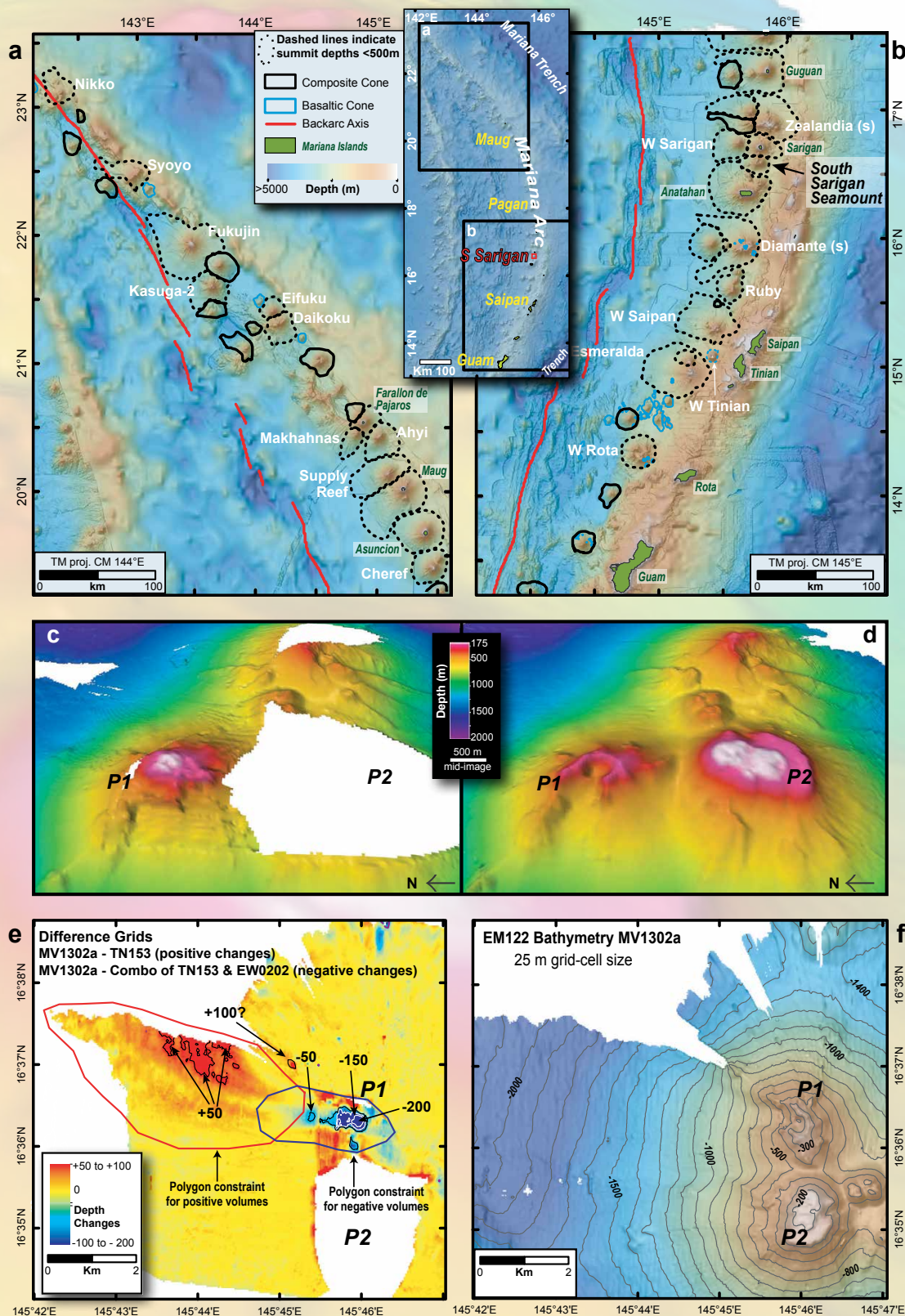


Figure 1. Maps showing the regional setting and details of the South Sarigan eruption site. The inset between the top panels locates the two maps. (a) Northern Seamount Province of the Mariana arc (Bloomer et al., 1989). Seamounts with summit depths < 500 m have dashed outlines. (b) Seamounts of the Southern Seamount Province indicating the location of South Sarigan Seamount. (c) Fledermaus © 3D image made from a combination of pre-eruption 2002 and 2003 bathymetry, view looking east toward the summit of South Sarigan Seamount. P1 and P2 are, respectively, the eruption site and the larger summit peak that was unsurveyed before 2013. Note P1's dome shape. (d) Fledermaus © 3D image made from post-eruption 2013 bathymetry, view looking east toward the summit of South Sarigan Seamount. Note the new crater on peak P1 and new bathymetry for peak P2, shown as a shallow flat white area. (e) Depth change map. Positive depth changes were determined by differencing the 2003 (TN153) bathymetry data with the 2013 (MV1302) bathymetry grid. The red polygon constrains the area used to calculate positive volumes. Negative depth changes were determined by differencing a combined grid of 2002 (EW0202) and 2003 (TN153) bathymetry data with the 2013 (MV1302) bathymetry grid. The blue polygon constrains the area used to calculate negative volumes. Contours represent 50 m depth change intervals; note negative depth change numbers at and near P1 where the crater is located and positive depth change contours downslope and west of the crater. (f) Post-eruption 2013 bathymetry map of South Sarigan Seamount with 100 m contours.

station in Palau (Green et al., 2013). After a short (~ 3 hour) quiescent period, the paroxysmal explosive events on May 29 produced the largest peak-to-peak hydro-acoustic signals and another large infrasound event (Green et al., 2013; Searcy, 2013). The final phase also generated a small tsunami with up to ~ 3 m runup on nearby Sarigan Island and 4–5 cm measured on tide gauges in Saipan, located about 270 km SSW (McGimsey et al., 2010). A biology field party on Sarigan Island (11 km to the north) heard a loud noise and observed an eruption plume rising from the ocean. The eruption plume was tracked by satellite, reaching ~ 12 km into the atmosphere and triggering a volcanic ash advisory statement for air traffic from the Washington Volcanic Ash Advisory Center. The overlying water column apparently prevented most of the mass flux of the eruption from breaching the ocean surface, consistent with satellite and other observations that the atmospheric plume was mostly vapor (McGimsey et al., 2010). This event is one of the few documented submarine eruptions originating from a water depth > 100 m that have breached the sea surface (Mastin and Witter, 2000; Kano, 2003; Carey et al., 2014).

TYPES OF SUBMARINE ERUPTION HAZARDS

Although most submarine eruptions occur along the mid-ocean ridge in deep water and without any impact on society (Rubin et al., 2012), there are significant numbers of potentially hazardous shallow submarine volcanoes above oceanic hotspots and along volcanic arcs within subduction zones. When compared to mid-ocean ridges, these volcanoes, particularly those along the volcanic arcs, are characterized by more explosive eruptions due to their shallower depths, higher volatile contents, and more viscous magmas. Most of the hundreds of seamounts in these settings are in the western Pacific, Mediterranean, and Caribbean areas (e.g., Mariana arc shown in Figure 1a,b). The large majority of these submarine volcanoes have poorly known geologic histories and hazards.

Historically, the major regional (up to hundreds of kilometers) hazard associated with island and/or submarine eruptions has been tsunamis (Latter, 1981; Mastin and Witter, 2000; Paris et al., 2013). The large “volcanic tsunami” generated during the paroxysmal eruptions of Krakatau and Thera (Santorini) were responsible for mass fatalities (Latter,

1981). Various causal mechanisms have been debated for these tsunamis, including submarine caldera collapse, pyroclastic flow surges into the ocean, and underwater explosions. The largest tsunami associated with the paroxysmal eruption of Thera was likely caused by rapid submarine caldera formation (McCoy and Heiken, 2000). The mechanism for the Krakatau tsunami remains controversial, although numerical wave modeling by Nomanbhoy and Satake (1995) favors an underwater explosive origin. Maeno et al. (2006) modeled tsunami inundations along the southern Kyushu (Japan) coast from a large submarine caldera collapse at offshore Kikai volcano 7,300 years ago. They determined that the amount of inundation is strongly dependent on the rate of caldera collapse. Large tsunamis can also be caused by very large flank failures on submarine volcanoes or hybrid (subaerial/submarine) failures from landslides associated with the collapses of island flanks. We will not address this class of hazard in this paper because it is not necessarily directly related to submarine eruptions and is covered elsewhere in this special issue (see Watt et al., 2014).

Locally hazardous tsunamis have also been generated from smaller underwater volcanic explosions such as those at Myōjin-shō (a shallow submarine volcano on the Izu-Ogasawara arc, south of Japan) in the early 1950s (Dietz and Sheehy, 1954). These types of volcanic tsunamis have also been reported from submarine eruptions near Ritter Island (Papua New Guinea) and Kickem Jenny volcano in the Caribbean (Beget, 2000). Submarine eruptions that breach the sea surface can threaten vessels, air traffic (from the ash cloud), and even nearby land masses. This direct hazard is exemplified by the tragic loss of the

Robert W. Embley (robert.w.embley@noaa.gov) is Senior Research Scientist, National Oceanic and Atmospheric Administration, Pacific Marine Environmental Laboratory, Newport, OR, USA. **Yoshihiko Tamura** is Principal Scientist, Japan Agency for Marine-Earth Science and Technology (JAMSTEC), Yokosuka, Japan. **Susan G. Merle** is Senior Research Assistant, Cooperative Institute for Marine Resources Studies, Oregon State University, Newport, OR, USA. **Tomoki Sato** is Technical Support Staff Member, JAMSTEC, Yokosuka, Japan. **Osamu Ishizuka** is Senior Scientist, Geological Survey of Japan of the Advanced Industrial Science and Technology Agency, Tsukuba, Japan, and Visiting Senior Scientist, JAMSTEC, Yokosuka, Japan. **William W. Chadwick Jr.** is Professor, Cooperative Institute for Marine Resources Studies, Oregon State University, Newport, OR, USA. **Douglas A. Wiens** is Professor, Department of Earth and Planetary Sciences, Washington University, St. Louis, MO, USA. **Patrick Shore** is Computer Specialist/Lecturer, Department of Earth and Planetary Sciences, Washington University, St. Louis, MO, USA. **Robert J. Stern** is Professor of Geosciences, University of Texas at Dallas, Dallas, TX, USA.

Japanese hydrographic vessel *No. 5 Kaiyo Maru* during investigations of Myōjin-shō volcano in 1952 (Niino, 1952; Dietz and Sheehy, 1954). Such eruptions can also produce large pumice rafts and sometimes build cones that reach into very shallow water and construct ephemeral islands that can be navigational hazards and that often disappear due to wave erosion (Vaughan et al., 2007; Carey et al., 2014). Rapid discharge of magmatic gases into the overlying water column is a potential submarine volcanic hazard above very shallow seamounts because sufficiently high gas concentrations can cause a loss of buoyancy for vessels (similar to the hazard caused by blowouts while drilling for hydrocarbons; Hovland and Gudmestad, 2001). Degassing episodes can occur even without accompanying eruptive activity either suddenly by tectonic triggering (Esposito et al., 2006) or from a slow buildup of magmatic gas in a submarine crater, a potential hazard recently identified at Kolumbo submarine volcano in the Aegean Sea (Carey et al., 2013).

The ocean acts as a damper for most submarine eruptions. Increased hydrostatic pressure at depth reduces gas exsolution and the relative high density and viscosity of water (versus air) rapidly reduces the velocity of pyroclastic material ejected during an eruption. The maximum depth we need to consider for submarine eruption hazards depends partly on the type of hazard, and presumably is directly related to the eruption's Volcanic Explosivity Index (see Discussion section below). Until recently, this depth was thought to be ~ 500 m (Mastin and Witter, 2000) to generate explosive and tsunami hazards, at least for all but the very largest submarine eruptions. However, a recent

widespread pumice raft and atmospheric plume formed above Havre Seamount (Kermadec arc) during its 2012 eruption, apparently from a source at > 700 m depth (Carey et al., 2014), underscoring our poor understanding of the depth limit below which submarine volcanoes are no longer a threat at the surface.

PRE- AND POST-ERUPTION BATHYMETRY OF SOUTH SARIGAN SEAMOUNT

During the past decade, there has been a dramatic increase in exploration and research on the intra-oceanic arcs (produced by the subduction of one oceanic plate beneath another) of the western Pacific by various groups using multibeam and side-scan sonars for broad-scale mapping and remotely operated vehicles for in situ studies (Embley et al., 2007, 2008). These efforts have only begun to assemble the geologic history of these hundreds of seamounts (Figure 1a,b), but the new mapping does provide a baseline that will help to document future submarine eruptions and slope failures. Differencing of pre- and post-event bathymetric surveys has been very effective in studying recent volcanic eruptions along mid-ocean ridges, on submarine volcanoes over hotspots, and along intra-oceanic arc submarine volcanoes (Rubin et al., 2012).

The available pre-eruption multibeam bathymetric surveys of South Sarigan Seamount from 2002 (Atlas Hydrosweep DS-2 multibeam, cruise EW0202) and 2003 (Simrad EM300 multibeam, cruise TN153) were incomplete, leaving a data gap over the shallow main peak (marked as P2 on Figure 1c). A single multibeam swath (EW0202) barely covered the north peak (marked as P1 on Figure 1c), the purported location of the 2010 eruption (McGimsey et al., 2010; Searcy,

2013). That survey shows a dome-shaped summit rising up to ~ 184 m water depth (Figure 1c). A post-event survey in February 2013 (Simrad EM122 multibeam, cruise MV1302) reveals that a breached crater, 350 m in diameter, and with up to ~ 200 m relief, had formed on the northern peak in the interval since the 2002 survey (P1 on Figure 1d,f). We are assuming that all the depth changes occurred as the result of the May 2010 eruptions because available seismicity records from stations on the nearby islands of Sarigan and Anatahan do not show any significant activity in the vicinity of South Sarigan Seamount except for the period of 2010 described above (Cheryl Searcy, Alaska Volcano Observatory, *pers. comm.*, 2014).

To quantify the changes that took place during the eruption, we used the MB-system © to create difference grids between the 2013 multibeam bathymetric data grid (MV1302a) and the two older data sets (2002 EW0202 and 2003 TN153). The resulting map (Figure 1e) shows a substantial area of negative depth change (up to ~ -200 m deeper on post-eruption survey) at and west of the summit of the northern peak (labeled P1 on Figure 1d,f). It also shows a smaller-magnitude but larger area of positive depth change (shallower on post-eruption survey) on the western flank of the seamount directly downslope of the breached crater (up to ~ +50 m). The negative depth change area includes the crater and a zone extending onto the upper flank. The deficit on the upper flank is probably the result of mass wasting likely induced by loading and/or earthquake triggering associated with the 2010 eruption seismicity episode. We interpret the positive depth change area as a large mass of material added to the slope during the 2010 eruptions.

Depth change volumes were calculated with QPS Fledermaus © software. Using the MV1302a/TN135 depth change grid, a volume for the downslope deposit (there is not complete coverage so this is only an estimate) is $\sim 1.7 \times 10^8 \text{ m}^3$. Calculating the volume lost from the summit area by differencing a grid that combines the two older surveys with the MV1302a grid yields a volume of $\sim 6.8 \times 10^7 \text{ m}^3$. This makes the deposit volume about 2.5 times the volume of the summit deficit. As discussed further below, the greater volume of the flank deposit relative to the summit deficit is consistent with the deposit being a combination of slope failure and juvenile volcanic products.

OBSERVATIONS AND SAMPLING AT THE ERUPTION SITE

Following the discovery of the summit crater and downslope deposit, two dives with the Japan Agency for Marine-Earth Science and Technology (JAMSTEC) remotely operated vehicle (ROV) *Hyper-Dolphin* explored and sampled both the crater and the western deposit in June 2013 (Tamura et al., 2013; Figure 2a). Dive HPD-1533 (Figure 2b) began at 409 m water depth on a sandy, boulder-strewn seafloor near the base of a steep scarp; the ROV then moved north to northeast up the wall to the crater rim at $\sim 239 \text{ m}$ water depth. The northeast wall of the crater is faced by a series of jointed andesite flows and dikes (Tamura et al., 2013; Figure 2c). There was white veining and/or streaking commonly on the outcrops (Figure 2d). This could be elemental sulfur, which can appear light-colored under water due to absorption of yellow wavelengths in seawater over short distances. Several small sediment-covered benches break the slope of the crater wall. Near the top

of the wall and on the crater's rim, an extensive white filamentous microbial mat covered boulders and outcrops (Figure 2e). This microbial mat is probably sustained by a diffuse (barely discernible on the video) hydrothermal flow. There were no observations of vent-endemic macrofauna communities and no indicators of active high-temperature venting. The crater floor and wall seen on this traverse did not “look” young—everything was coated with dull brown/orange material, and sediments were thicker on the benches and on the crater floor. No young-looking lava flows were observed, although this dive traversed very little of the crater floor. However, one indicator that the crater has relatively “young” seafloor is the lack of sessile macrofauna on the outcrops, such as the deep corals commonly found on the hard substrata of the shallow seamounts of the Mariana arc (Rogers, 2007).

Dive HPD-1534 traversed the middle of the thickest portion of the downslope deposit, from 1,540 to 1,355 m water depth (Figure 2f). The seafloor was strewn with large, jointed-appearing, partially buried andesite blocks embedded in sandy pumiceous volcanoclastic deposits (Figure 2g). Three push cores taken at $\sim 0.5 \text{ km}$ intervals along the $\sim 1.0 \text{ km}$ traverse recovered pumiceous gravel that was crudely size sorted away from the summit. The deposit's surface and the blocks were covered with a thin orange-brown deposit or precipitate.

Several factors control the explosivity of volcanic eruptions, but water- and silica-rich magmas tend to erupt more violently than water- and silica-poor magmas. Arc magmas in general are water rich, $\sim 4\% \text{ H}_2\text{O}$ in basaltic magmas (Plank et al., 2013), and we assume that this is also the case for South Sarigan.

South Sarigan magmas are intermediate in silica content (Figure 2h), dominated by olivine-bearing two pyroxene andesites (Tamura et al., 2013). These andesites are found as pumices in the cores and as lava blocks on the deposit surface and on crater-wall outcrops. Andesitic pumice (which could be from the eruption) and lava blocks (which are probably older lavas flows) show similar limited ranges of SiO_2 (54–56 wt % and 54–58 wt %, respectively) and MgO contents (4.0–6.5 wt % and 3.5–6.0 wt %, respectively; Figure 2h). K_2O contents of the lava blocks ranges from 0.2–0.8 wt %, whereas pumices contain 0.6–0.8 wt % K_2O . Incompatible trace element ratios further highlight the narrower range of pumice compositions (Figure 2h) compared to the lavas. Pumices have a much smaller range of Ba/Th (300–350) and La/Sm (2.0–2.2) than do lava blocks ($\text{Ba/Th} = 250\text{--}700$ and $\text{La/Sm} = 1.4\text{--}2.5$, respectively). These values are similar to those of primitive basalts from Pagan Volcano in the Mariana arc to the north (Figure 1a,b, inset) reported by Tamura et al. (2014). Because of the abundance of andesite and the absence of other lithologies in the suite collected in the crater (HPD-1533) and in the downslope deposit (HPD-1534), we conclude that the recent eruptions of South Sarigan—including that of May 2010—have been dominated by andesite.

From the observations and samples made during the dives in June 2013, we can also conclude the following: (1) the geology of the crater is consistent with it having formed during the 2010 event, (2) some of the jointed andesite lavas from the disruption/collapse of the summit are present on the surface of the downslope deposit, (3) the location (within the downslope positive depth change zone), size grading, and distinct

chemistry of the pumiceous deposit are consistent with it being an eruptive product of the 2010 event, (4) the heterogeneous chemistry of the lava blocks indicate that they represent more than one lava flow/eruption episode, consistent with them being part of the former summit, and (5) some latent heat from the eruption/intrusion was still being diffusely discharged at the summit in June 2013. The ubiquitous orange coating on the surface of the deposit is enigmatic, but could be either iron oxides precipitated (possibly by microbial activity) during the cooling of the deposit or the last layer of (altered?) ash from the water column plume generated during the eruption.

DISCUSSION AND IMPLICATIONS FOR SUBMARINE VOLCANIC HAZARDS

The results from bathymetry remapping and seafloor observations are broadly consistent with the interpretation of the seismic and hydroacoustic data (Green et al., 2013; Searcy, 2013). During a precursory period beginning on May 27, eruptions and intrusions produced water-borne acoustic T-phases and volcanic tremor as pressure built up beneath the summit. The underwater explosion(s) on May 29, 2010, detected 8,000 km away off western Canada (Green et al., 2013), marked the paroxysmal eruption. The roughly two-day eruption period probably produced the breached summit crater along with juvenile pyroclastic and hydroclastic deposits. Volume calculations derived from the bathymetric difference grids show that the deposit contains ~ 2.5 times the volume of that removed from the summit. This observation and the relative chemical homogeneity of the

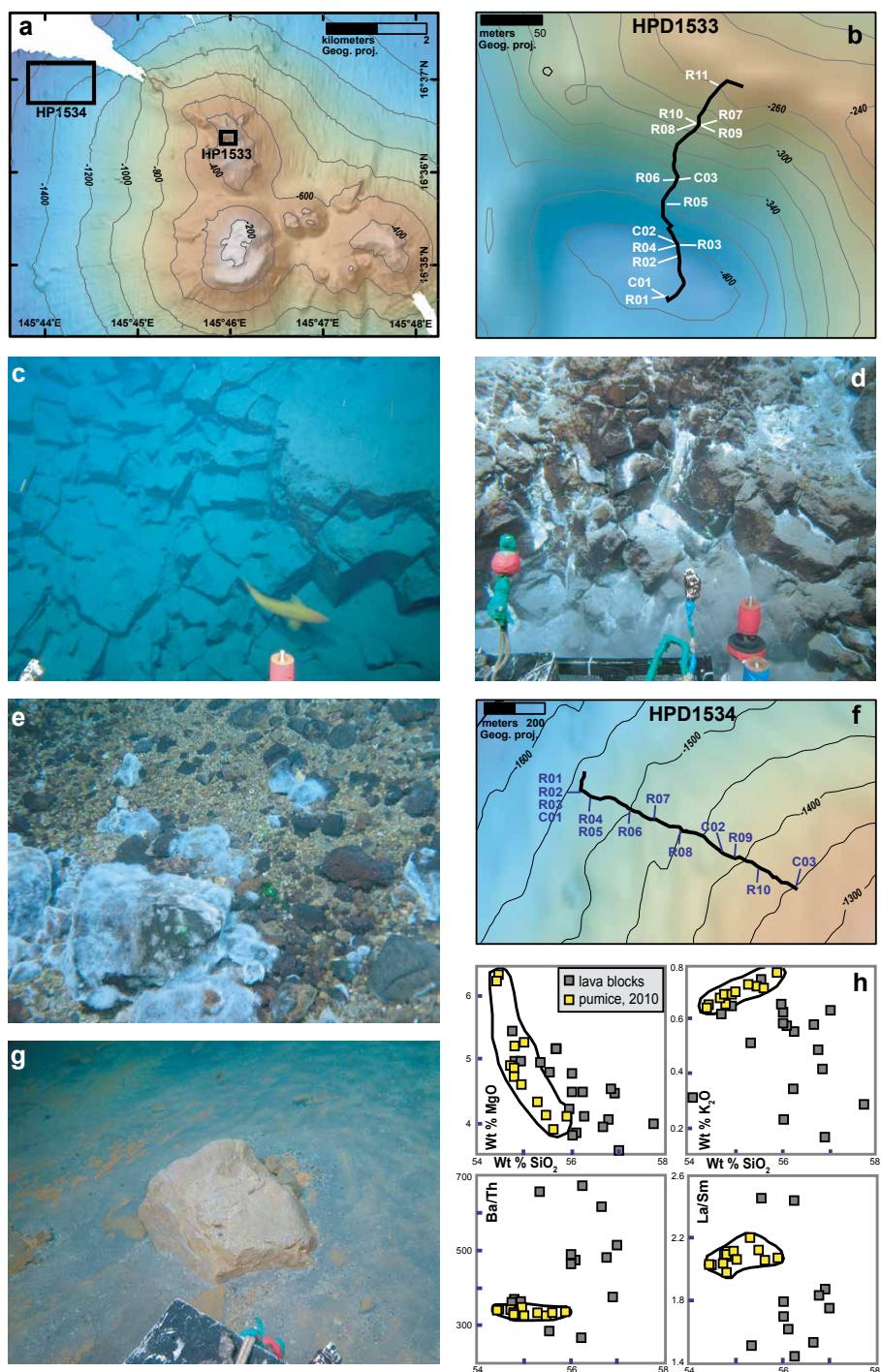


Figure 2. Results from June 2013 dives with JAMSTEC Hyper-Dolphin remotely operated vehicle (ROV) at South Sarigan Seamount. The photos were taken with a SEAMAX digital still camera (DSC) mounted on the ROV. (a) Bathymetric map (200 m contours) of South Sarigan Seamount showing locations of dives HPD-1533 and HPD-1534. (b) Dive track of HPD-1533 on the summit crater wall with collection of rock and core samples designated "R" and "C." (c) Photo of andesite outcrop on the north wall of the crater (358 m water depth). (d) SEAMAX DSC photo shows white staining on fractures in the crater wall (278 m water depth) that is possibly elemental sulfur. (e) SEAMAX DSC photo shows the microbial mat that covers boulders near the top/rim of the crater (240 m water depth). (f) Dive track of HPD-1534 on downslope deposit with rock and core sampling indicated as in Figure 2b. The bathymetry underlay has a 20 m contour interval. (g) SEAMAX DSC photo of a large columnar-jointed andesite block (1,435 m water depth). (h) Variation of MgO and K₂O (top boxes) and Ba/Th and La/Sm ratios (bottom boxes) with SiO₂ (wt %) for downslope pumice recovered from cores (yellow squares) and andesites from downslope blocks and summit crater wall (gray squares). Pumices are from dives HPD-1534 and andesite blocks are from HPD-1533 and HPD-1534.

downslope pumice fragments compared to the lava blocks imply that at least some of the young flank deposits represent juvenile erupted material. These analyses also indicate that the large jointed blocks observed on the surface of the downslope deposit originated from the summit. However, much more of the summit material is presumably buried in the deposits (up to ~ 50–75 m thick in places) and/or lie upslope from the dive area. The downslope deposits are volcanoclastic that likely include juvenile material, such as pumice, and fragmental material (including the large blocks) produced by disintegration and collapse of the summit.

How does the South Sarigan eruption compare to arc andesite eruptions on land? The only commonly used index for the size of volcanic eruptions is the Volcanic Explosivity Index (VEI). However, most parameters used as criteria for the VEI (e.g., height of eruption cloud) don't directly apply to the South Sarigan event because the indices were developed for a solid Earth/atmosphere interface rather than a solid Earth/ocean/atmosphere eruption. At this point, we know that: (1) there was a short (~ 2 days) eruptive period culminating with a large explosive event, (2) a large crater (~ 350 m diameter) formed sometime during the eruption, and (3) the deposit volume was 2.5 times larger than the volume of the crater and material removed by summit collapse. The explosive nature of the eruption and the estimated juvenile deposit volume of $\sim 1 \times 10^8 \text{ m}^3$ places the eruption within the moderate-large to large (VEI = 3–4) category, roughly comparable to the destructive Mt. Pelée eruption (Siebert et al., 2010). The size of the deposit is also consistent with that inferred from the hydroacoustic records by

Green et al. (2013).


The South Sarigan event is one of the first instances of an explosive, relatively deep, submarine eruption that breached the surface ocean and for which we have quantitative data for the size and extent of the cratering event and deposits to match with seismic and hydroacoustic monitoring information. Submarine craters the size of the one formed during the eruption of South Sarigan are relatively common on seamounts along intra-oceanic arcs (Figure 1a,b shows those along the Mariana arc). This event, and a deeper and much larger event at Havre Seamount in the Kermadec arc in 2012 (Carey et al., 2014), underscores how little is known of the eruption history of most submarine arc volcanoes. Many Mariana arc submarine edifices are complex composite volcanoes with multiple summits. Eruptions of the size of the South Sarigan, although not historically well documented, are probably common on a geologic time scale. How many of these seamounts are dormant versus extinct and how do we recognize the difference? Most intra-oceanic arc, hotspot, and other potentially active submarine volcanoes have only minimal sampling of dredged rocks of undetermined age. There is clearly a need not only to sample these sites but also to conduct in situ studies of the slopes and summits in order to reconstruct their geologic histories.

Monitoring submarine volcanoes is also a prescient issue. At present, monitoring of submarine volcanic activity is challenging because the global seismic arrays are mostly limited to coverage of continental areas and usually don't record far-field volcanic seismicity. For the foreseeable future, we will probably depend on hydroacoustic and island seismometer arrays to monitor

submarine volcanism. At present, these are limited to just a few sites in the Indian, Pacific, and Atlantic Oceans. The existing arrays can only detect some submarine eruptions, and the locations are not always robust, particularly in complex areas. This was exemplified by a submarine eruption in the northern Mariana arc that occurred while this paper was being finalized (May 2014). The locations of the seismic events using the far-field hydroacoustic arrays were not precise enough to definitively locate the eruption site, although, at least initially, it is thought to be Ahyi (<http://www.volcano.si.edu/volcano.cfm?vn=284141>), a seamount lying southeast of the island of Farallon de Pajaros (Figure 1a). Clearly, we need to work toward a monitoring system that will more effectively cover the most potentially hazardous submarine volcanoes. There is much work to do if we are to better understand the hazards associated with submarine arc volcanoes.

ACKNOWLEDGMENTS

We are grateful to the NOAA Vents Program (now Earth Oceans Interaction Program) and the NOAA Office of Ocean Exploration and Research for long-term funding support of the Mariana arc explorations. JAMSTEC provided funding for Y. Tamura, the *Hyper-Dolphin* ROV dives, and the support vessel *Natsushima*. This work was supported in part by the JSPS Grant-in-Aid for Scientific Research [(B) (23340166)]. The 2002 and 2013 mapping cruises were supported by the National Science Foundation (2013 cruise OCE-0841074). We thank the crews and science teams on the research vessels *T.G. Thompson*, *Ewing*, *Melville*, and *Natsushima* for their hard work at sea. We are grateful to J. White, M. Perfit,

G. McGimsey, and J. Chaytor for their helpful reviews and C. Searcy and D.N. Greene for informative discussions about the history of seismic and hydro-acoustic monitoring in the southern Mariana arc. PMEL contribution number 4139. 

REFERENCES

- Beget, J.E. 2000. Volcanic tsunamis. Pp. 1,005–1,014 in *Encyclopedia of Volcanology*. H. Sigurdsson, ed., Academic Press, San Diego.
- Bloomer, S.H., R.J. Stern, and N.C. Smoot. 1989. Physical volcanology of the submarine Mariana and volcano arcs. *Bulletin of Volcanology* 51:210–224, <http://dx.doi.org/10.1007/BF01067957>.
- Carey, R., R. Wysoczanski, R. Wunderman, and M. Jutzeler. 2014. Discovery of the largest historic silicic submarine eruption. *Eos Transactions, American Geophysical Union* 95(10):157–159, <http://dx.doi.org/10.1002/2014EO190001>.
- Carey, S., P. Nomikou, K.C. Bell, M. Lilley, J. Lupton, C. Roman, E. Stathopoulou, K. Bejelou, and R. Ballard. 2013. CO₂ degassing from hydrothermal vents at Kolumbo submarine volcano, Greece, and the accumulation of acidic crater water. *Geology* 41:1,035–1,038, <http://dx.doi.org/10.1130/G34286.1>.
- Dietz, R.S., and M.J. Sheehy. 1954. Transpacific detection of Myojin volcano explosions by underwater sound. *Geological Society of America Bulletin* 65:941–956, [http://dx.doi.org/10.1130/0016-7606\(1954\)65\[941:TDOMVE\]2.0.CO;2](http://dx.doi.org/10.1130/0016-7606(1954)65[941:TDOMVE]2.0.CO;2).
- Embley, R.W., E.T. Baker, D.A. Butterfield, W.W. Chadwick Jr., J.E. Lupton, J.A. Resing, C.E.J. de Ronde, K. Nakamura, J.F. Dower, and S.G. Merle. 2007. Exploring the submarine ring of fire: Mariana Arc, western Pacific. *Oceanography* 20(4):68–79, <http://dx.doi.org/10.5670/oceanog.2007.07>.
- Embley, R.W., C.E.J. de Ronde, and J. Ishibashi. 2008. Introduction to special section on active magmatic, tectonic, and hydrothermal processes at intraoceanic arc submarine volcanoes. *Journal of Geophysical Research* 113, 808S01, <http://dx.doi.org/10.1029/2008JB005871>.
- Espósito, A., G. Giordano, and M. Anzidei. 2006. The 2002–2003 submarine gas eruptions at Panarea volcano (Aeolian Islands, Italy): Volcanology of the seafloor and implications for the hazard scenario. *Marine Geology* 227:119–134, <http://dx.doi.org/10.1016/j.margeo.2005.11.007>.
- Green, D.N., L.G. Evers, D. Free, R.S. Matoza, M. Snellen, P. Smets, and D. Simons. 2013. Hydroacoustic, infrasonic and seismic monitoring of the submarine eruptive activity and sub-aerial plume generation at South Sarigan, May 2010. *Journal of Volcanology and Geothermal Research* 257:31–43, <http://dx.doi.org/10.1016/j.jvolgeores.2013.03.006>.
- Hovland, M., and O.T. Gudmestad. 2001. Potential influence of gas hydrates on seabed installations. In *Natural Gas Hydrates: Occurrence, Distribution, and Detection*. C.K. Paull and W.P. Dillon, eds, Geophysical Monograph Series, American Geophysical Union, Washington, DC, <http://dx.doi.org/10.1029/GM124p0307>.
- Kano, K. 2003. Subaqueous pumice eruptions from their products: A review. In *Explosive Subaqueous Volcanism*. J.D.L. White, J.L. Smellie, and D.A. Clague, eds, Geophysical Monograph Series, American Geophysical Union, Washington, DC, <http://dx.doi.org/10.1029/140GM14>.
- Latter, J.H. 1981. Tsunamis of volcanic origin: Summary of causes, with particular reference to Krakatoa, 1883. *Bulletin of Volcanology* 44:467–490, <http://dx.doi.org/10.1007/BF02600578>.
- Maeno, F., F. Inamura, and H. Taniguchi. 2006. Numerical simulation of tsunamis generated by caldera collapse during the 7.3 ka Kikai eruption, Kyushu, Japan. *Earth, Planets, and Space* 58:1,013–1,024, <http://www.terrapub.co.jp/journals/EPS/abstract/5808/58081013.html>.
- Master, L.G., and J.B. Witter. 2000. The hazards of eruptions through lakes and seawater. *Journal of Volcanology and Geothermal Research* 97:195–214, [http://dx.doi.org/10.1016/S0377-0273\(99\)00174-2](http://dx.doi.org/10.1016/S0377-0273(99)00174-2).
- McCoy, F.W., and G. Heiken. 2000. Tsunami generated by the Late Bronze Age eruption at Thera (Santorini), Greece. *Pure and Applied Geophysics* 157:1,227–1,256, <http://dx.doi.org/10.1007/s000240050024>.
- McGimsey, R.G., C.A. Neal, C.K. Searcy, J.T. Camacho, W.B. Aydlott, R.W. Embley, F.A. Trusdell, J.F. Paskievitch, and D.J. Schneider. 2010. The May 2010 submarine eruption from South Sarigan Seamount, Northern Mariana Islands. Paper presented at 2010 Fall Meeting of the American Geophysical Union, December 13–17, Abstract T11E-07.
- Niino, H. 1952. Explosions of Myojin Reef. *Kagaku Asahi* December:3–23.
- Nomanbhoy, N., and K. Satake. 1995. Generation mechanism of tsunamis from the 1883 Krakatau eruption. *Geophysical Research Letters* 22:509–512, <http://dx.doi.org/10.1029/94GL03219>.
- Paris, R., A.A. Switzer, M. Belousova, A. Belousov, B. Ontowirjo, P.L. Whelley, and M. Ultvova. 2013. Volcanic tsunami: A review of source mechanisms, past events and hazards in Southeast Asia (Indonesia, Philippines, Papua New Guinea). *Natural Hazards* 70:447–470, <http://dx.doi.org/10.1007/s11069-013-0822-8>.
- Plank, T., K.A. Kelley, M.M. Zimmer, E.H. Hauri, and P.J. Wallace. 2013. Why do mafic arc magmas contain ~ 4 wt% water on average? *Earth and Planetary Science Letters* 364:168–179, <http://dx.doi.org/10.1016/j.epsl.2012.11.044>.
- Rogers, A.D., A. Baco, H. Griffiths, T. Hart, and J.M. Hall-Spencer, eds. 2007. Corals on seamounts. Pp. 141–169 in *Seamounts: Ecology, Fisheries & Conservation*. T.J. Pitcher, T. Morato, P. J.B. Hart, M.R. Clark, N. Haggan, and R.S. Santos, eds, Blackwell Publishing, Singapore.
- Rubin, K.H., S.A. Soule, W.W. Chadwick Jr., D.J. Fornari, D.A. Clague, R.W. Embley, E.T. Baker, M.R. Perfit, D.W. Caress, and R.P. Dziak. 2012. Volcanic eruptions in the deep sea. *Oceanography* 25(1):142–157, <http://dx.doi.org/10.5670/oceanog.2012.12>.
- Searcy, C. 2013. Seismicity associated with the May 2010 eruption of South Sarigan Seamount, northern Mariana Islands. *Seismological Research Letters* 84(6):1,055–1,061, <http://dx.doi.org/10.1785/0220120168>.
- Siebert, L., T. Simkin, and P. Kimberly. 2010. *Volcanoes of the World*, 3rd ed. University of California Press, Berkeley, CA.
- Tamura, Y., R.W. Embley, A.R. Nichols, O. Ishizuka, S.G. Merle, W.W. Chadwick Jr., R.J. Stern, T. Sato, D.A. Wiens, and P. Shore. 2013. ROV *Hyper-Dolphin* survey at the May 2010 eruption site on South Sarigan Seamount, Mariana Arc. Paper presented at the 2013 Fall Meeting of the American Geophysical Union, San Francisco, California, Abstract V31G-02.
- Tamura, Y., O. Ishizuka, R.J. Stern, A.R. Nichols, H. Kawabata, Y. Hirahara, Q. Chang, T. Miyazaki, J.-I. Kimura, R.W. Embley, and Y. Tatsumi. 2014. Mission immiscible: Distinct subduction components generate two primary magmas at Pagan Volcano. *Journal of Petrology* 55:63–101, <http://dx.doi.org/10.1093/petrology/egt061>.
- Vaughan, R.G., M.J. Abrams, S.J. Hook, and D.C. Pieri. 2007. Satellite observations of new volcanic island in Tonga. *Eos Transactions, American Geophysical Union* 88(4):37–41, <http://dx.doi.org/10.1029/2007EO040002>.
- Watt, S.F.L., P.J. Talling, and J.E. Hunt. 2014. New insights into the emplacement dynamics of volcanic island landslides. *Oceanography* 27(2):46–57, <http://dx.doi.org/10.5670/oceanog.2014.39>.